Line strengths, self-broadening, and line mixing in the 20 0 0←01 1 0(Σ←Π)Q branch of carbon dioxide

Adriana Predoi-Cross, Caiyan Luo, R. Berman, J. R. Drummond, and A. D. May

Citation: The Journal of Chemical Physics **112**, 8367 (2000); doi: 10.1063/1.481480
View online: http://dx.doi.org/10.1063/1.481480
View Table of Contents: http://scitation.aip.org/content/aip/journal/jcp/112/19?ver=pdfcov
Published by the AIP Publishing

Line strengths, self-broadening, and line mixing in the $20^00 \leftarrow 01^10$ ($\Sigma \leftarrow \Pi$) Q branch of carbon dioxide

Adriana Predoi-Cross, Caiyan Luo, R. Berman, J. R. Drummond, and A. D. May[a)]
Department of Physics, University of Toronto, Toronto, Canada M5S 1A7

(Received 22 October 1999; accepted 24 February 2000)

Using a difference frequency spectrometer we have measured the $Q(2)$ to $Q(38)$ $20^00 \leftarrow 01^10$, $\Sigma \leftarrow \Pi$ transitions of carbon dioxide at 296 K and pressures up to 15 kPa. These low pressure spectra were analyzed using both the Voigt model, and an empirical line shape that blends together a hard collision model and a speed dependent Lorentzian profile. The broadening coefficients were obtained with an accuracy of 1% or better. The low density or first order low pressure line mixing parameters were also determined. We have compared both our measured low pressure line-mixing parameters and the complete band spectrum at high pressures with those predicted by a relaxation matrix calculated from an EPG fitting law. Spectra at the highest pressures were recorded using both the difference frequency spectrometer and an FTIR spectrometer, the temperature for the latter experiments being 303 K. The vibrational band intensity and linear pressure shift of the branch as a whole were also measured. © *2000 American Institute of Physics.* [S0021-9606(00)01519-1]

INTRODUCTION

Carbon dioxide, because it is both a strong IR absorber and is uniformly mixed at altitudes up to 80 km, is the constituent most commonly used for satellite remote sensing of the temperature of the Earth's atmosphere.[1] As in any remote sensing technique, the measurements rely upon having available a correct model of the absorption profiles. Typically, the line parameters reported in the literature were obtained in the laboratory by fitting the spectral profiles to a Lorentz or Voigt line shape. The drawback here is that such profiles may not correctly model the real absorption profile of an isolated line.[2]

A second problem, from the view of remote sensing, is that even with the appropriate spectral model, the parameters required to generate the profile may not have been accurately measured. This is the case for many of the very closely spaced lines of some of the Q branch lines in CO_2 perturbed by N_2 and O_2. In such cases the practice[3] has been to assume that the linewidths are branch independent and to set them equal to measured widths of lines belonging to other branches where the lines are more widely spaced and the parameters more easily measured.

There is a third problem which goes beyond the question of determining the appropriate line profile, line strength and the broadening and shifting parameters for isolated lines. For closely spaced lines, coupling may become important and the band can not be represented as a sum of isolated lines.[4–6] The impact of this interference between the lines (line mixing) on temperature retrievals has already been stressed by several authors.[7–9] For instance, Edwards and Strow[9] estimated that omitting line mixing in the retrieval algorithm may result in errors in the measured temperature as high as 10 K in certain measurements. For CO_2, understanding and quantifying line mixing is very important as it is the ''thermometer'' for most atmospheric sounding systems.[1]

In this study, we are concerned with the physics of pure CO_2 gas. This case is applicable to the planetary atmosphere of Venus, which is almost pure CO_2. The case of terrestrial atmosphere is more complex as the gas is diluted to less than 0.04% by N_2 and O. This study of the pure gas system is a necessary precursor to the study of the mixed gas system strictly applicable to the earth's atmosphere and such future studies are required. However, many of the results can be immediately applied to remote sounding computations since even an approximate treatment of line mixing is superior to ignoring the effect entirely.

The physics of line mixing is well understood.[4–6] However, quantifying the effect is not trivial. Coupling between the lines is described by a relaxation matrix. For an isolated line only the diagonal elements or broadening coefficients are required and a band may be described on a line by line basis. When the lines overlap, all elements of the relaxation matrix are important and are required to describe the band as a whole. There are no direct measurements of the off-diagonal elements of a relaxation matrix for any gas. One source of information about the off-diagonal elements comes from the measurement of the so-called mixing coefficients, in the weak mixing limit.[10,11] Experimentally this requires an accurate measure of the asymmetry of individual lines at low pressure. For closely spaced Q branch lines ($\Delta J = 0$) this means very low pressures where the limiting width is the Doppler width. Consequently, reliable mixing coefficients can only be obtained if the instrumental resolution is at least 10 times smaller and preferably 100 times smaller than the Doppler width. For the 2130 cm^{-1} Q branch of CO_2 at atmospheric temperatures the Doppler width is about 120 MHz (FWHM). Thus direct measurements of weak line mixing in this system requires a resolution at least on the order of 20

a)Author to whom correspondence should be addressed. Department of Physics, University of Toronto, 60 St. George St., Toronto, Canada M5S 1A7. Electronic mail: dmay@physics.utoronto.ca

MHz and preferably higher. Currently, the only spectrometers capable of such high resolution are diode spectrometers[12] and difference frequency laser spectrometers.[13] These can achieve resolutions on the order of 1 MHz. Line shifts in atmospheric gases are typically much smaller than linewidths. Nevertheless, with a resolution of 1 MHz it is possible to measure line shifts. Here we use a difference frequency spectrometer to measure linewidths and asymmetries and the overall band shift of the 2130 cm^{-1} Q branch of pure CO_2 at low pressures. The lines are analyzed in terms of a Voigt profile and spectral profile first introduced by Henry *et al.*[12] and adapted to include line mixing by Berman *et al.*[2,13] and Predoi-Cross *et al.*[14] At high pressures, where severe overlapping of the lines occurs and resolution is not a problem, we have used an FTIR spectrometer to record the band. Here, we examine the suitability of an EPG ''law'' [8,9,11] to relate the broadening to both the mixing when the lines weakly overlap and to the spectra at high pressures.

EXPERIMENTAL DETAILS

We have described our difference frequency laser spectrometer in earlier publications.[15,16] Here we outline its main features. Infrared radiation in the 2.5 to 5.5 μm region is obtained by overlapping the beams from a frequency-stabilized Argon ion laser and a Coherent 699-29, R6G dye laser and mixing them in a nonlinear $LiIO_3$ crystal. The infrared power is normalized by dividing the infrared beam and monitoring the input and output signals of an absorption cell with two identical LN_2 cooled InSb detectors. To avoid etalonning effects in the optics, the cell and detectors had CaF_2 windows mounted at the Brewster angle while the $LiIO_3$ crystal was antireflection coated. The maximum variation of the empty cell transmission (baseline signal) was one part in 500 for a 1 cm^{-1} scan. The frequency measuring subsystem has as principal component a temperature stabilized, scanning Fabry–Perot interferometer and a frequency stabilized He–Ne laser to monitor the variation of the frequency of both the dye and Argon ion laser. Using this experimental setup we can achieve a resolution of about 1 MHz (3×10^{-5} cm^{-1}) and a signal-to-noise ratio close to 1500:1 for a 1 second integration time.

In the present experiment at low pressures, we have used a temperature controlled 4 m long gas cell. The cell middle point temperature (296 K) was controlled with a precision of $\pm$0.4 K and measured using thermocouples. We have tried to minimize the temperature gradients at the cell ends by attaching additional heating coils to the end flanges. As a check we have compared the thermocouple readings with the temperature determined spectroscopically by measuring the ratio of line intensities of two Q branch lines. This ratio depends upon the rotational gas temperature and the transition dipole strengths. For line strengths we have used the values reported in the HITRAN database.[3] Using this simple method we have confirmed that the rotational gas temperature agrees within 0.5 K with the reading of the mid-cell thermocouple.

Most measurements with the difference frequency spectrometer were made at pressures ranging from 0.7 to 15 kPa. The gas pressure was measured with an MKS 120 AA capacitance manometer, calibrated by the manufacturer to an absolute accuracy of 0.05% of the full scale reading. The calibration of the MKS gauge at atmospheric pressure was checked with a barometer and the zero point was adjusted using a vacuum gauge.

The high pressure spectra presented in this work were recorded using a Bomem DA8.003 Fourier transform spectrometer with a 0.5 mm aperture. With this setting, the instrumental linewidth (0.004 cm^{-1}) was much smaller than the width of the collapsed Q branch. For the FTIR spectra we used a 25.0 cm, temperature-controlled cell equipped with CaF_2 windows. The temperature was measured and stabilized at 303 K. Spectra with a signal-to-noise ratio in excess of 1000:1 were recorded from 1 to 20 atm. In all cases, the gas was precision Aquarator ($<$7 ppm methane) and supplied by Matheson. To provide a comparison between the two sets of measurements, a few spectra in the neighborhood of 1 atm and lower were recorded with both spectrometers. No systematic difference between the two sets was detected.

Figure 1(a) shows the FTIR transmission spectrum of CO_2 from 2060 to 2140 cm^{-1} as measured at a pressure of 97.49 kPa. There are three strong Q branches in this region. The branch at 2077 cm^{-1} was studied by Berman *et al.*[13] Here we report on the branch at 2130 cm^{-1}. In a future publication we will report on the branch at 2093 cm^{-1}. Figure 1(b) shows on an expanded frequency range the $\Sigma\leftarrow\Pi$ branch at 2130 cm^{-1} observed with the FTIR spectrometer at several pressures between 1 and 19 atm. Figure 1(c) shows the same spectrum observed with the difference frequency spectrometer but over a range of pressures from 0.67 to 13.34 kPa (100 kPa=1 atm). Below 15 kPa the lines are generally well resolved (line mixing is weak) and have a width (HWHM) on the order of 100–300 MHz. Since the resolution limit of the FTIR spectrometer is 120 MHz it is clear that it could not yield accurate line shapes at such low pressures. On the other hand, the difference frequency spectrometer with a resolution on the order of 1 MHz is ideal for accurate line shape studies of this band at such pressures. This would continue to hold true even if the pressure were reduced further since the limiting Doppler width is calculated to be 60 MHz (HWHM). As we shall see, below 15 kPa line mixing is weak for this Q branch. Consequently our paper naturally divides into two sections. The first part deals with spectra recorded at low densities with the difference frequency spectrometer. These spectra are analyzed in terms of isolated lines or lines showing weak mixing. The second section deals with measurements at higher pressure made with either the difference frequency or the FTIR spectrometer. The analysis at high pressures consists of seeing how well the analysis at low pressure may be extrapolated to interpret the spectra in the strong mixing limit. Since this paper deals with a number of aspects of line shapes, to aid the reader, we make liberal use of titles and subtitles to separate the different areas.

ANALYSIS

Figure 1(c) showed sample CO_2 spectra of the 2130 cm^{-1} Q branch at pressures below 15 kPa. Only J even lines exist for this branch since only J even states are found in the

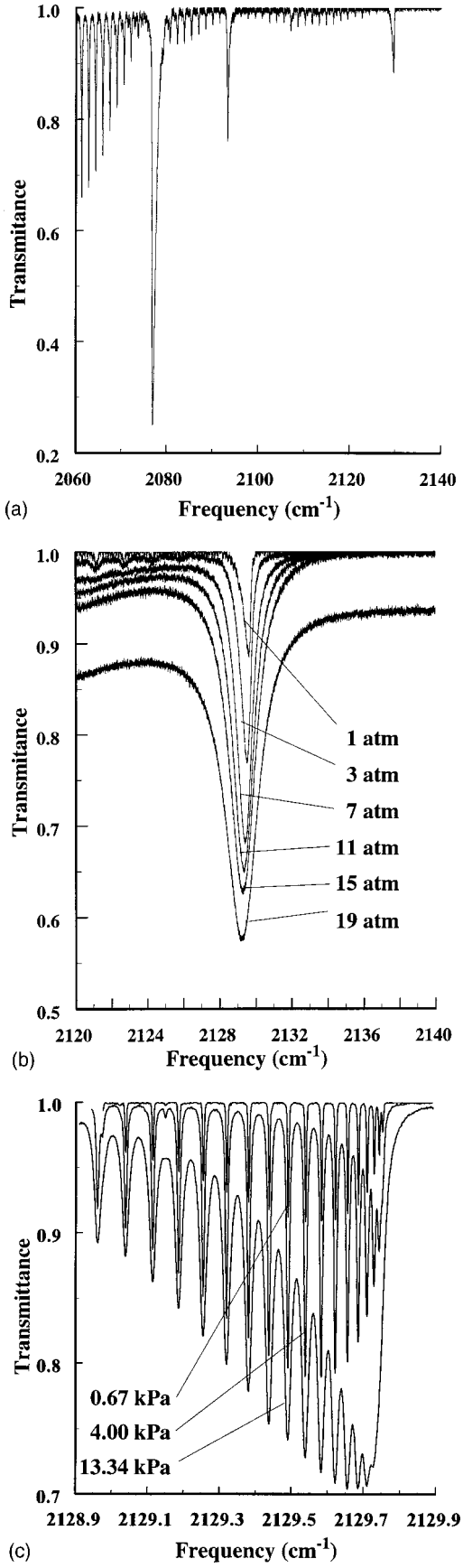

FIG. 1. Absorption spectra of pure CO_2, (a) FTIR spectrum showing bands in the 2100 cm^{-1} region at 1 atm, (b) FTIR spectra of the Q branch at 2130 cm^{-1} at several pressures above 1 atm, and (c) difference frequency spectra of the Q branch at 2130 cm^{-1} at a fraction of an atm (1 atm=100 kpa).

upper level. It is convenient to analyze the band as a whole, rather than on a line by line basis. We do this in an iterative and progressive manner. First we analyze the data up to 5 kPa using approximate values of weak mixing coefficients. The approximate mixing coefficients are derived from broadening data for the CO_2 Q branch at 2077 cm^{-1}. This yields reliable experimental values of the line strengths and a good first order approximation to the experimental widths. In a second iteration, we use the strengths from the first step and fit the band, for pressures up to 15 kPa, for accurate values of the widths and approximate experimental values of the first order mixing parameters. In a final iteration we estimate the second order mixing terms[7] using our broadening coefficients and refit again for the experimental widths and now accurate experimental values of the first order mixing parameters. We have found that this method of analysis converges rapidly and is convenient when fitting an entire Q branch. The final results are accurate experimental values of the line strengths, broadening coefficients and weak mixing parameters. The band shift, being small, is less accurately determined.

For the first step in the analysis we required an *estimate* of the first order mixing parameters. We follow a common practice and construct a relaxation matrix starting from the low density width of the lines and an EPG law[8,9,11] for the rates of relaxation of the rotational states. The EPG law gives the collisional transfer rate, κ_{jk}, from a rotational state k to a higher rotational state j as

$$\kappa_{jk}=a[|\Delta E_{jk}|/B_0]^{-b}\exp[-c|\Delta E_{jk}|/B_0], \tag{1}$$

where ΔE_{jk} is the rotational energy difference between the two states and B_0 is the rotational constant. The parameters to be optimized are a, b, and c. Since the molecular system is in thermodynamic equilibrium, the rates of population transfer must satisfy the detailed balance condition

$$\rho_k\kappa_{jk}=\rho_j\kappa_{kj} \tag{2}$$

where ρ_k is the population of the rotational state, k. Equation (2) fixes the rates for downward transitions, relative to the rates for the upward transitions.

There is a question as to the relative values of the rotational relaxation rates in the two different vibrational states. Following Edward and Strow[9] and Berman *et al.*[13] we take κ_{jk} to be the rates for the vibrational state with only J even, here the upper level for the 2130 cm^{-1} Q branch. For the lower state we take the rate between even J states as $\beta\kappa_{jk}$ and the J odd to J even as $(1-\beta)\kappa_{jk}$. This model keeps the rates, out of a given, even J state in both the lower and upper vibrational levels, nearly the same.

We must now establish the relationship(s) between the population relaxation rates and the elements of the relaxation matrix W. In a pure random phase approximation one would set the diagonal elements of W, or width of a line, to one-half of the sum of the total rates out of the lower and upper levels involved in the transition. The off-diagonal elements of the relaxation matrix would then be one-half the sum of the single rates between the two upper levels and the two lower levels of the corresponding transitions. Such a model would automatically yield interbranch $(P-Q-R)$ mixing and sat-

isfy the sum rule for a column of the relaxation matrix. As in Refs. 9 and 11, we depart from a pure random phase model by ignoring interbranch mixing. However, we still fix the widths or diagonal elements according to

$$W_{kk}=(1/2)\left\{\sum_j \kappa_{jk}\right\} + (1/2)\left\{\sum_j \beta\kappa_{jk}+\sum_j (1-\beta)\kappa_{jk}\right\}, \tag{3}$$

where k is even. On the right hand side, the first two terms have j even while the third term has j odd. The curly brackets separate the contributions associated with the upper and lower vibrational states. It is clear, given a,b,c, β and the spacing of the rotational states, that the broadening coefficients may be calculated. Conversely, given the broadening coefficients the set of constants a,b,c and β may be determined or fitted in a least squares sense. At the first stage we lack experimental values of the broadening coefficients for this Q branch. However, as is well known, the widths are relatively insensitive to the particular Q branch. Initially we use both the broadening parameters and the value of β reported in Ref. 13 for the branch at 2077 cm^{-1}. We also require the rotational state energies. These we take from the HITRAN database.[3] The estimated values of a, b, and c are 51.085×10^{-3} cm^{-1}/atm, 0.258 167 and 0.002 64, respectively.

So far we have outlined the connection between broadening coefficients or diagonal elements of the relaxation matrix and the rotational relaxation rates. For the first fitting of our experimental profiles we require an estimate of the first order line mixing. This requires, among other things, the off-diagonal elements of the relaxation matrix, W_{jk}. Continuing to follow Refs. 9 and 13, we assume that the relationship between the off-diagonal elements of W and the rotational relaxation rates to be given by

$$W_{jk}=-\beta\kappa_{jk} \tag{4}$$

when the Π state is involved. This is justified on the basis of calculations performed by Green.[17]

Having established our model for the relaxation matrix, the next step is to describe the spectral profile(s) used for the band. If we neglect the translational motion and assume the broadening and shifting is speed independent, then up to second order in the components of the relaxation matrix, the absorption coefficient may be written[7] in the form

$$\alpha(\nu)=\sum_i (N/\pi)S_i\{P\gamma_i(1-PZ_i+P^2G_i)+PY_i(\nu-\nu_i - P\delta_i-P^2H_i)\}/\{(\nu-\nu_i-P\delta_i-P^2H_i)^2+(P\gamma_i)^2\}, \tag{5}$$

where the broadening coefficient, γ_i equals the real part of W_{ii} (expressed in per atm) and the shifting coefficient, δ_i, equals the imaginary part of W_{ii}. P is the pressure, N is the number of active molecules per unit volume, and ν_i is the free molecule transition frequency. If the integrated line intensity, S_i, is given in $cm^{-1}/(molecule/cm^2)$, then frequencies in Eq. (5) must be in cm^{-1}. The complex weak mixing coefficient Y_i+iZ_i is given by

$$Y_i+iZ_i=\sum_k \mu_i\mu_k(W_{ik}\rho_k+W_{ki}\rho_i)/S_i\nu_{ik}, \tag{6}$$

where $\nu_{ik}=\nu_i-\nu_k$ and W_{ik} is an off-diagonal element of the relaxation matrix. To be consistent with the gap law model introduced above we must take Z_i equal to zero. It is clear from Eq. (5) that each line consists of a Lorentzian line shape plus an asymmetric term proportional to the associated dispersion curve. In the weak mixing limit ($G_i=H_i=0$) the strength of the asymmetric term grows linearly with pressure relative to the symmetric component. This is a well-known signature of weak mixing.

For the first few Q branch lines the Rosenkranz[10] or weak mixing approximation is inadequate at 15 kPa. As implied by the iterative fitting routine outlined above we correct the experimental profiles by estimating the contribution made by the second order or Smith's terms, G_i and H_i and subtracting them from the experimental data. The intensity factor, G_i is given[7] by

$$G_i=\sum_k W_{ik}W_{ki}/\nu_{ki}^2-\left\{\sum_k (\mu_k/\mu_i)W_{ki}/\nu_{ki}\right\}^2 + 2\sum_k (\mu_k/\mu_i)W_{ki}W_{ii}/\nu_{ki}^2 - 2\sum_k\sum_l (\mu_k/\mu_i)W_{ki}W_{li}/\nu_{ki}\nu_{li}. \tag{7}$$

The quadratic shift coefficient H_i is given[7] by

$$H_i=\sum_k W_{ki}W_{ik}/\nu_{ki}. \tag{8}$$

Now Eq. (5), as it stands, is inadequate for atmospheric modeling. It neglects Doppler broadening and Dicke narrowing and it neglects speed dependent broadening and shifting. For CO_2, collisional shifting is weak and almost constant across the branch (see, for example, Ref. 13). Thus we may safely ignore speed dependent shifting. It is common practice in atmospheric modeling to neglect Dicke narrowing and speed dependent broadening and to consider only Doppler and collisional broadening. The corresponding Voigt profile including line mixing is obtained from Eq. (5) by convolution with a Gaussian profile. We refer to this profile as the V_{wm} band profile. The main reason for considering it is historical. A more realistic model that includes Dicke narrowing and speed dependent broadening is needed.

To include speed dependent broadening and Dicke narrowing for isolated lines, Henry *et al.*[12] convolved the speed dependent Lorentzian with the hard collision model for the translational motion. Since an entire band, including weak mixing, has the form of a sum of isolated line profiles plus the associated dispersion curve it was possible for Berman *et al.*[2,13] and Predoi-Cross *et al.*[14] to generalize the form of Henry *et al.*[12] They constructed a profile for an entire band, including weak mixing, speed dependent broadening and Dicke narrowing. We refer to this model as the HC_v (band)

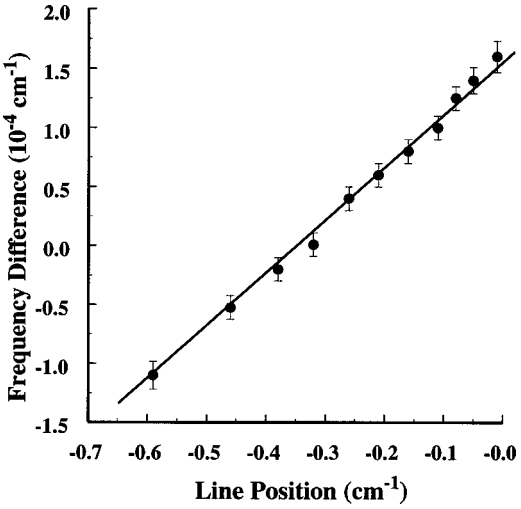

FIG. 2. Difference between measured frequencies in the 2130 cm^{-1} Q branch lines and corresponding HITRAN96 values plotted versus line position.

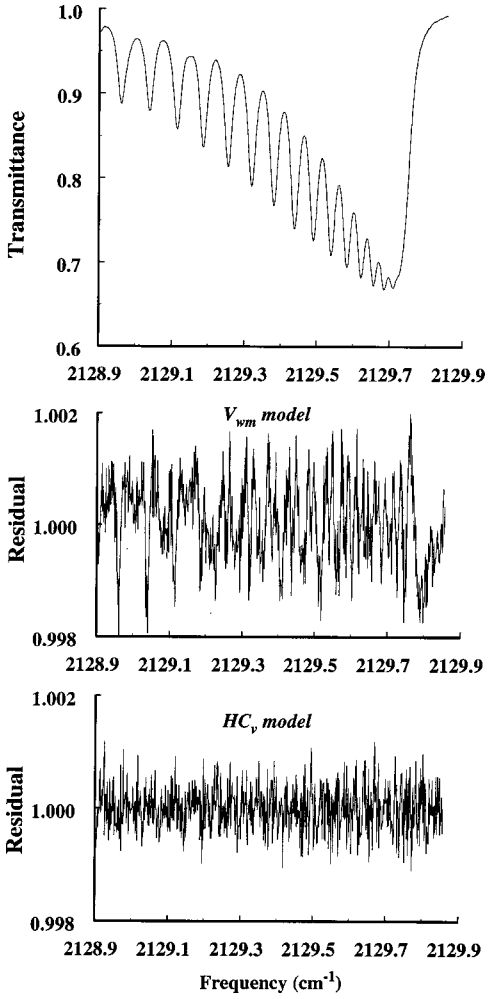

FIG. 3. Transmittance (I/I_0) for the CO_2, Q branch at 2130 cm^{-1}, measured with the difference frequency spectrometer at 14.55 kPa and 298 K. Also shown are the residuals ($T_{obs}-T_{fit}$) when the V_{wm} or the HC_v model is used in the fitting routine.

profile. For the expert reader, we note this is distinct from the well-known speed dependent hard collision model of Rautian and Sobelman.[18] Berman *et al.*[2] have shown that the HC_v model gives a realistic description of an isolated line all the way from the low density Doppler limit up to the extreme Dicke limit where the direct contribution of the translational motion to the width may be ignored. Most important, of all the models examined, they showed that it gives the most physical result for the width, i.e., proportional to pressure. The hard collision model for the translational has as input parameter, the diffusion constant. Here we use the mass diffusion constant.[19] This yields a value of 10.9 atm^{-1}for the so-called narrowing parameter commonly used in the literature.[20] Finally, Berman *et al.*[21] have recently given an algorithm for calculating a speed-dependent Lorentzian in terms of two carefully chosen speed independent or simple Lorentzians. Thus it is a simple matter to implement a model with weak mixing, Dicke narrowing and with speed-dependent broadening by adding two equations of the form given above for the band absorption coefficient [Eq. (1)] each convolved with a Gaussian profile. A method for establishing the relative strengths and relative widths of the two speed-independent Lorentzians to best describe a speed dependent Lorentzian has been given by Berman *et al.*[21] In their terminology the value of q used here for all of the lines was 6.00.

RESULTS (0 TO 15 kPa)

Frequency calibration

In analyzing the low pressure results, we found small systematic differences existed between the measured relative frequencies and those listed in Hitran96.[22] Figure 2 shows a plot of the difference in frequency plotted as a function of the frequency of the line. Note the disagreement is only a few times 10^{-4} cm^{-1}, i.e., less than 10 MHz. The difference can be explained by a change, during realignment, in the length of the interferometer used to monitor the frequency of the dye and argon ion lasers. To correct for this we have recalibrated the interferometer spacer using the Hitran96 values for the frequencies of the lines. For all further analysis we used the corrected experimental frequency axis.

Spectral fits

The simplest test of a spectral profile is the accuracy with which it reproduces the experimental profiles. In Fig. 3 we present an experimental spectrum at 14.55 kPa and the residual from the fit with the both the V_{wm} and the HC_v model. Without the frequency corrections there would be very large residuals at each line. More important is the fact that the residuals are much larger for the V_{wm} model than for the HC_v model. This is understandable. At 14.55 kPa Dicke narrowing is important and the Voigt profile is no longer appropriate. As HC_v converges to V_{wm} at low densities the two residuals must converge at lower pressures. At 5 kPa both profiles reproduce the experimental profiles equally well. Thus we inter-compare fitted values only for results below 5 kPa. As we will see below the frequency shifts are very small and except for the very low J lines, line mixing is

TABLE I. Frequencies in cm^{-1} and line strength in units of 10^{-24} cm^{-1}/(molecule/cm^2) of CO_2 at 2130 cm^{-1} and 298 K.

J	v in cm^{-1}	Present $S_Q(J)$[a]	experiment $S_Q(J)$[b]	Ref. 23 $S_Q(J)$[c]	HITRAN 96 $S_Q(J)$[d]
38	2128.880 38	1.98(3)	1.99(4)	1.98	1.97
36	2128.961 04	2.53(3)	2.51(4)		2.47
34	2129.039 07	3.09(3)	3.07(4)	3.01	3.04
32	2129.114 22	3.73(3)	3.70(6)		3.68
30	2129.186 11	4.39(3)	4.36(5)	4.34	4.37
28	2129.254 65	5.11(3)	5.08(6)		5.08
26	2129.319 50	5.81(3)	5.78(4)		5.80
24	2129.380 49	6.48(3)	6.45(4)	6.58	6.48
22	2129.437 44	7.09(3)	7.06(5)		7.09
20	2129.490 14	7.54(3)	7.51(5)	7.64	7.58
18	2129.538 44	7.89(3)	7.86(5)	7.97	7.91
16	2129.582 18	7.99(3)	7.96(6)	8.15	8.04
14	2129.621 25	7.88(3)	7.84(7)	8.06	7.93
12	2129.655 52	7.48(3)	7.44(8)	7.71	7.56
10	2129.684 91	6.85(4)	6.81(8)	7.05	6.92
8	2129.709 48	5.99(4)	5.94(8)	6.17	6.01
6	2129.728 81	4.98(7)	4.88(8)		4.86
4	2129.742 18	3.53(9)	3.59(9)		3.51
2	2129.752 13	1.96(9)	2.13(10)		2.00

[a]As determined by fitting with the HC_v model.
[b]As determined by fitting with the V_{wm} model.
[c]As determined by fitting with a Voigt profile.
[d]As determined by fitting with a Voigt profile and averaged over several bands.

unimportant below this pressure. Thus we actually intercompare only the intensities and the broadening coefficients determined from fitting HC_v and V_{wm}.

Intensities

The first results to appear from the iterative and progressive fitting routine are the line intensities. Line mixing can alter the apparent intensities even when the lines appear relatively well resolved, i.e., Z_i may not be zero experimentally. Thus accurate individual line intensities emerge from an analysis of the data below a few (~5) kPa. Table I lists the two values of the line strengths as determined from the two fitted profiles. Examination of the table reveals that the line strength determined from the best fit V_{wm} profile is marginally smaller than that from the HC_v model. The results should be the same and indeed they overlap within the quoted error bars. Also included in the table are the values as measured by Rinsland *et al.*[23] and the values tabulated in HITRAN96.[22] These were determined by fitting profiles to a simple Voigt profile. At the low densities used here we may ignore the difference between a simple Voigt profile and V_{wm}. Essentially, our results agree with the HITRAN values within our quoted errors.

Neglecting interbranch mixing, the integrated band intensity is independent of the degree of line mixing. From the medium pressure spectra ($5 \leqslant P \leqslant 15$ kPa) we can determine the total band strength. In the fitting process we fixed the relative line strengths to the values obtained from spectra at lower pressures and floated the overall vibrational Q branch intensity. The dominant source of error in our result arises from baseline uncertainty. The uncertainties in the pressure and cell length are negligible.

TABLE II. Total strength in units of 10^{-24} cm^{-1}/(molecule/cm^2) of the CO_2 Q branch at 2130 cm^{-1} and 298 K.

References	$S_Q(2130\ cm^{-1})$
Present measurements	209.36(4)
Rinsland *et al.* (Ref. 23)	213.2(5)
Rothman *et al.* (Ref. 24)	119.0
HITRAN (Ref. 22)	209.93

In Table II we compare our vibrational band intensity with Fourier transform measurements of several other groups.[22–24] The error quoted in Table II for our results is twice the fit error. Our measurement does not agree within the stated error limits with the two Fourier transform measurements but is close to the mean value tabulated in HITRAN96.[22] Given the higher frequency resolution of the difference frequency system and better baseline determination than in the other experiments, we believe our strength measurement to be the most accurate value for this band.

Widths and broadening coefficients

As an example, Fig. 4 shows, as a function of pressure, a plot of the widths, determined by fitting the profiles to the HC_v model. When speed dependence of the broadening is included in the fitting profile, the term ''width'' loses precise meaning. The width reported here is the Boltzman averaged width and is generally designated as Γ_m in the literature.[21] In spite of the fact that the model is mathematically flawed (strictly speaking, one cannot write the spectrum as a convolution[6]) we see from Fig. 4 that the width satisfies the commonly accepted view that it should be proportional to pressure. Thus we may define pressure broadening coefficients as the slope of the line which passes through zero, in plots of Γ_m versus pressure. We designate these as $\overline{\gamma}$. Similar

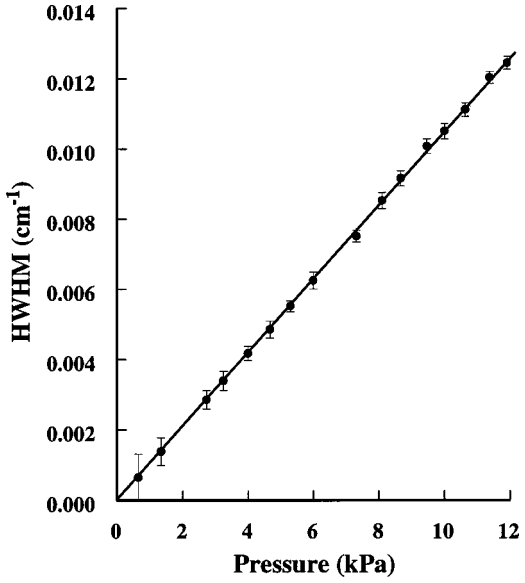

FIG. 4. Measured half-width (HWHM) as a function of pressure for the $Q(10)$ line. The error bars are the statistical values (one standard deviation) obtained from the fits to the HC_v profile. The solid line is the best fit straight line forced to pass through the origin.

TABLE III. Broadening coefficients of pure CO_2, in units of cm^{-1}/atm.

	Present results[b]		Ref. 13[c]	Ref. 11[d]	Ref. 25[e]	Ref. 20[f]	Ref. 22[g]
m[a]	4.7 μm	4.7 μm	4.8 μm	4.8μm	10.6 μm	4.3 μm	All bands
2	0.1276(45)	0.1317(12)	0.1243(17)	0.1343	0.119	0.1214	0.1228
4	0.1169(26)	0.1156(6)	0.1165(5)	0.1175	0.1162	0.1173	0.119
6	0.1128(30)	0.1078(8)	0.1129(5)	0.1137	0.1108	0.1124*	0.1141
8	0.1102(18)	0.1054(6)	0.1094(3)	0.1098	0.1074	0.1115	0.1116
10	0.1075(6)	0.1037(4)	0.1063(4)	0.107	0.1066	0.1074	0.1091
12	0.1044(4)	0.1014(4)	0.1037(3)	0.1072	0.1053	0.1042	0.1067
14	0.1021(4)	0.0998(4)	0.1018(3)		0.1025	0.1038	0.1043
16	0.1003(3)	0.0980(4)	0.0996(3)		0.1015	0.1009	0.102
18	0.0985(3)	0.0967(4)	0.0979(3)		0.0988	0.099	0.0998
20	0.0969(3)	0.0946(4)	0.0961(6)		0.0974*	0.0994	0.0977
22	0.0953(4)	0.0937(4)	0.0945(4)		0.0956	0.0973*	0.0956
24	0.0938(4)	0.0920(4)	0.0925(5)		0.0937	0.0959	0.0935
26	0.0921(4)	0.0904(4)	0.0906(5)		0.0902*	0.0917	0.0916
28	0.0903(4)	0.0887(4)	0.0886(7)		0.0869	0.0893*	0.0897
30	0.0884(5)	0.0868(4)	0.0867(6)		0.0885	0.0882	0.0878
32	0.0873(5)	0.0855(4)	0.0848(5)		0.0856	0.0882	0.086
34	0.0853(4)	0.0848(4)					0.0843
36	0.0831(4)	0.0833(4)					0.0826
38	0.0821(5)	0.0814(14)					0.081

[a]$m=j+1$ for the R branch, $m=-j$ for P branch, and $m=j$ for Q branch transitions. The P and R branch measurements are averaged as $\gamma=[\gamma_m+\gamma_{m+1}]/2$. The * indicates that either γ_m or γ_{m+1} was not available.
[b]The second column gives $\overline{\gamma}$, the broadening coefficient obtained using the HC_v model, and the third column gives the values for γ obtained using the V_{wm} profile.
[c]The Q branch measurements of Berman *et al.* (Ref. 13) were made at 301 K.
[d]Gentry and Strow's (Ref. 11) measurements were made at a single pressure and 296 K.
[e]The results of Dana *et al.* (Ref. 33) are from P and R branch measurements in the laser band region at 294 K.
[f]The results of Johns (Ref. 25) are from P and R branch measurements made in a hot band near 4.3 μm at 300 K.
[g]HITRAN96 [Rothman *et al.* (Ref. 22)] uses a collection of results and assumes the widths to be band and branch independent.

results (width proportional to pressure) were found when the profiles below 5 kPa were fit with V_{wm}. We designate the broadening coefficients determined in such a manner simply as γ. Since V_{wm} is almost identical to a sum of pure Voigt profiles at these pressures, these broadening coefficients may be compared with values obtained by other researchers who used a simple Voigt profile to fit individual lines.

We summarize in Table III our broadening coefficients for the 2130 cm^{-1} band and those measured by others[11,13,23,25,26] for a variety of Q branch lines. We see from the first two columns of broadening coefficients that the values resulting from fitting with a Voigt profile, γ, are systematically smaller than those obtained using the HC_v model, $\overline{\gamma}$. This is consistent with the observations of Berman *et al.*[2] As a consequence it is only reasonable to compare our Voigt results with the results of others, all of whom used a Voigt profile or at least a profile that neglected speed dependence. Figure 5 illustrates what is well known, viz that the broadening coefficients are largely band independent, an assumption made in compiling the HITRAN data base.

Line mixing coefficients

The last major result obtained from analyzing the low pressure data ($0 \leqslant P \leqslant 15$ kPa) is the weak mixing parameter, i.e., the combination, PY, of Eq. (5). We only use HC_v since V_{wm} does not well represent the isolated line spectral profile well over the entire pressure range, 0–15 kPa. If the isolated line is not well represented then there is confusion as to how much asymmetry is due to direct overlap of lines and how much is due to line mixing. The first test of the analysis, using HC_v, is the dependence of the strength of the mixing on pressure. Figure 6 shows plots, as a function of pressure, of the mixing parameter for the $Q(2)$ and $Q(20)$ lines. One way of interpreting the parameter is the ratio of the maximum amplitude of the dispersion or asymmetric component of the line to the amplitude of the symmetric component at line center. For the $Q(2)$ line it is already 20% at about 4 kPa. On the other hand, for the $Q(20)$ line it is only about 1/2% at the same pressure. We see in both cases that the mixing parameter is indeed proportional to the pressure. For each individual spectral line we have determined the mixing parameters, $Y(J)$ by a linear regression, forcing the fitted line to pass through the origin. These direct experimental measurements of line mixing are presented in Table IV. There we present two columns of results. One, experimental values obtained by neglecting the second order mixing terms, G and H and second, values obtained by correcting the data using our estimated values of G and H. We see from the table and from a plot of the results (Fig. 7) that the second order terms only make a significant contribution to the mixing for J values below about 10.

As is evident from Fig. 7 the line mixing coefficients vary considerably throughout the band, both in magnitude and sign. This is characteristic of line mixing in Q branches.

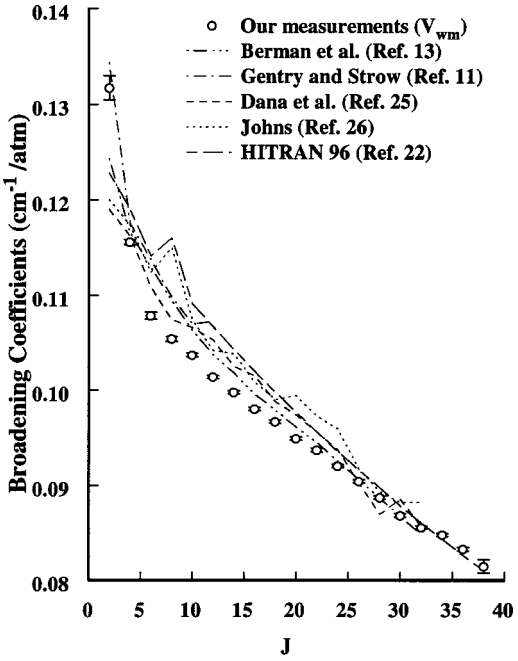

FIG. 5. Observed Q branch broadening parameters as a function of J. Open circles are the present results using V_{wm} to fit the spectra. The various lines show the results of other experimenters for a variety of branches (see Table II for details).

The strength of the mixing varies inversely as the frequency separation of the lines, which in Q branches changes quadratically with the rotational quantum number, J. The change in sign of the mixing coefficients is characteristic of mixing in general. It merely indicates the band as a whole is narrowing by collapsing to a point near the center of gravity of the band. In Fig. 7 we have plotted J increasing to the left. For this band, then, frequency decreases to the left in Fig. 7 just as it does in Fig. 1. This presentation makes a later discussion simpler.

Testing the EPC model

Above we used the broadening coefficients (diagonal elements of the relaxation matrix) to determine the constants of the EPG model. We then used the model to calculate all elements of the relaxation matrix. In the final iteration of the fitting routine the off-diagonal elements were used to estimate the second order or Smith's correction in order to generate improved experimental values of the weak mixing coefficients. We now ask how well the off-diagonal elements based on the EPG model are able to predict these experimental weak mixing coefficients. Included in Table IV are the estimated mixing coefficients for two different choices of β [see Eqs. (4) and (6)]. We see that $\beta=0.6$ gives the closest agreement between the experimental values and those estimated from a EPG law for the rotational relaxation rates and the assumed relations between these rates and the elements of the relaxation matrix. The values for the a, b, and c coefficients in Eq. (1) obtained for β equal to 0.6 are: 51.782 $\times 10^{-3}$ cm^{-1}/atm, 0.259 739 and 0.002 635, respectively. These differ little from our first estimate or from the values for the Q branch at 2077 cm^{-1}.[13] Also included in Table IV

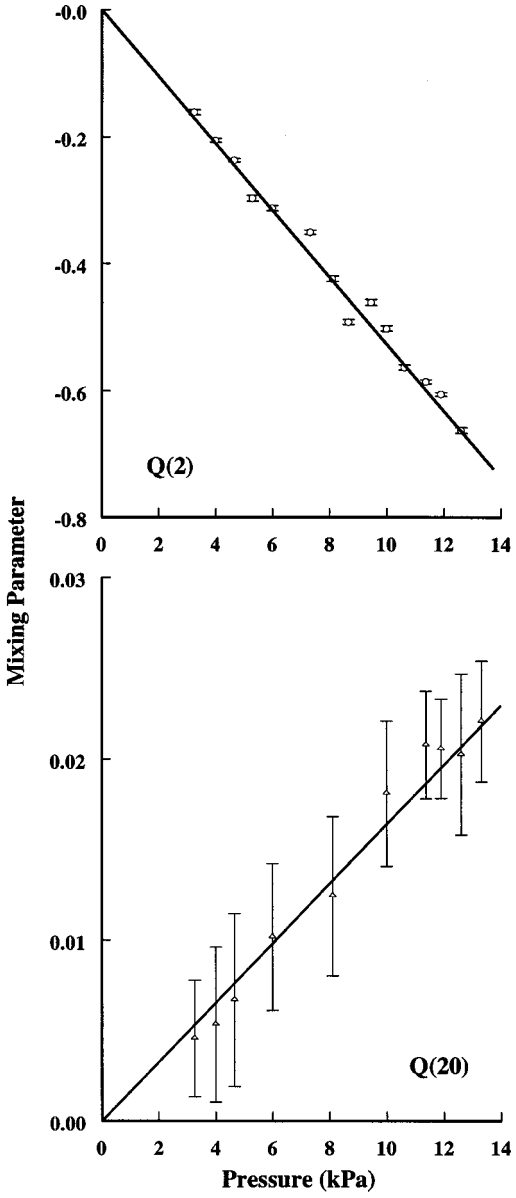

FIG. 6. Measured line mixing parameter for $Q(2)$ and $Q(20)$ as a function of pressure. The error bars are the statistical values (one standard deviation) obtained from the fits to the HC_v profile. The solid lines are linear regression fits to the data.

are the weak mixing coefficients as modeled by Strow *et al.*[27] Except for the $Q(4)$ line the latter are in agreement with our experimental values and our values based on an EPG law.

Assuming detailed balance between the off-diagonal elements of the relaxation matrix and the expression for the mixing coefficient allows one to deduce the sum rule, $\Sigma_i S_i Y_i = 0$.[28,29] We checked our experimental values for agreement with this sum rule and found $\Sigma_i S_i Y_i = -1.68\times 10^{-23} + 1.34\times 10^{-23} = -0.34 \times 10^{-23}$ cm^{-1}/(molecule/cm^2). This is significantly different from zero. It can be argued that the discrepancy arises from the neglect of interbranch mixing. The sum rule is supposed to be applied to the entire spectrum or at least to all interacting lines. Since a branch collapses towards its center of gravity, Fig. 7 reminds us that our sign convention is such that

TABLE IV. Weak line mixing coefficients, in units atm^{-1}, for transitions of the 2130 cm^{-1} Q branch of pure CO_2 at 298 K.

	Experimental		Calculated		
	a	*b*	*c*	*d*	*e*
J			$\beta=0.6$	$\beta=0.63$	$\beta=0.54$
2	−5.32(12)	−5.03(11)	−5.022	−5.296	−4.892
4	−1.80(4)	−1.43(4)	−1.493	−1.573	−0.950
6	−0.35(2)	−0.28(3)	−0.236	−0.248	−0.248
8	−0.038(8)	−0.08(2)	−0.006	−0.006	−0.012
10	0.078(9)	−0.006(10)	0.091	0.096	0.089
12	0.081(5)	0.048(5)	0.153	0.161	0.137
14	0.099(6)	0.087(9)	0.183	0.193	0.160
16	0.169(8)	0.143(9)	0.198	0.209	0.172
18	0.169(9)	0.161(9)	0.205	0.216	0.176
20	0.196(8)	0.179(5)	0.205	0.216	0.176
22	0.211(9)	0.200(6)	0.202	0.213	0.175
24	0.201(9)	0.198(5)	0.198	0.208	0.172
26	0.215(6)	0.206(6)	0.192	0.202	0.168
28	0.200(9)	0.206(4)	0.186	0.196	0.164
30	0.208(7)	0.196(9)	0.180	0.189	0.160
32	0.172(6)	0.187(5)	0.173	0.183	0.157
34	0.184(8)	0.172(5)	0.167	0.176	0.153
36	0.174(7)	0.165(4)	0.162	0.170	0.150

[a]Experimental results obtained by ignoring the second order or Smith (Ref. 7) terms.
[b]Experimental results obtained by correcting data for second order terms.
[c]Calculated coefficients from present broadening coefficients using a value for β of 0.6.
[d]Calculated coefficients from present broadening coefficients using a value for β of 0.63.
[e]Calculated coefficients using the expressions given in Ref. 27 for $\beta=0.54$.

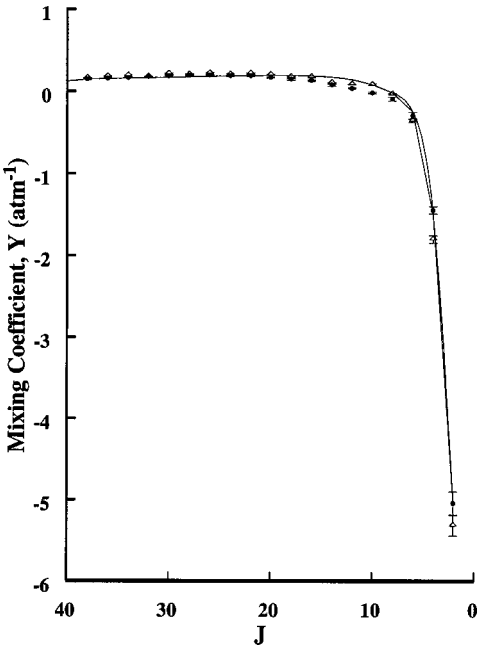

FIG. 7. Measured weak line mixing coefficients versus rotational quantum number, J. Open triangles are results obtained without correcting spectral data for second order mixing. Filled circles are mixing coefficients obtained with a second order correction based on an EPG law for the rotational relaxation rates. The error bars are obtained from the linear regressions of the line mixing parameters as a function of pressure. The smooth solid line is the value calculated from the EPG law and the broadening coefficients of this paper.

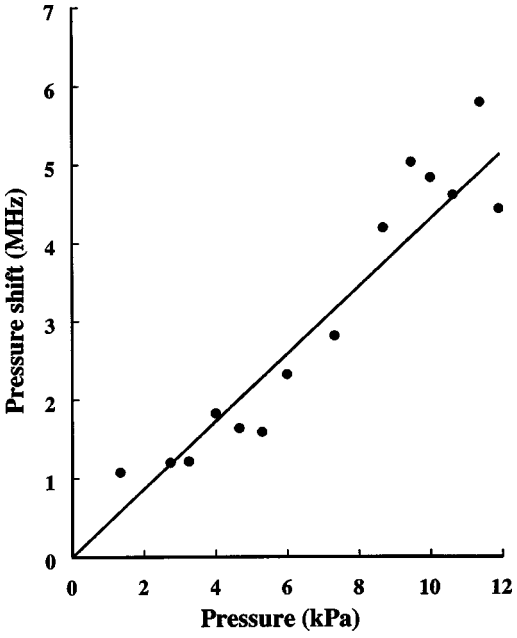

FIG. 8. Shift of the 2130 cm^{-1} Q branch as a function of pressure. The solid line is a straight regression fit that is used to define the position of the origin.

negative Y values pulls this band towards lower frequencies. Since interbranch mixing between the Q branch and the strong P branch at lower frequencies (see Fig. 1) will pull the Q branch towards it, it follows that the interbranch contribution to mixing in the Q branch will be negative. Thus a sum over only the Q branch lines is expected to be negative. This is the first piece of evidence that $P-Q$ branch mixing may not be ignored even at low pressures. If the discrepancy in the sum rule is due to interbranch mixing, then undoubtedly, it is the anomalously low intensity of the R branch with respect to the P branch that makes it possible to detect the effect in this Q branch.

Frequency shift (low pressures)

The fitting routine included the mean frequency of the band as a floated parameter. Figure 8 shows a plot of the frequency shift versus pressure. We see that it is linear in pressure. The fitted straight line shown in Fig. 8 has a slope (shifting coefficient) of $0.146\times10^{-3}\,cm^{-1}$/atm. This is of the same size but of opposite sign from that measured by Berman *et al.* for the Q branch at 2077 cm^{-1}. Perhaps this is explained by the fact that the character of the states involved (Σ and Π) are the same but the levels for the two transitions are inverted one with respect to the other.

RESULTS ($P\geqslant15$ kPa)

There are a number of interesting, and at the same time disturbing, features in the spectra as the pressure is increased beyond 15 kPa. Figure 9 shows a set of spectra at approximately 0.5, 1, 3, and 5 atmospheres compared to our calculated spectra. The calculated spectra use our relaxation matrix, as determined from the low pressure broadening coefficients and an EPG model for the relaxation of the rotational states. We follow the usual method of full inversion

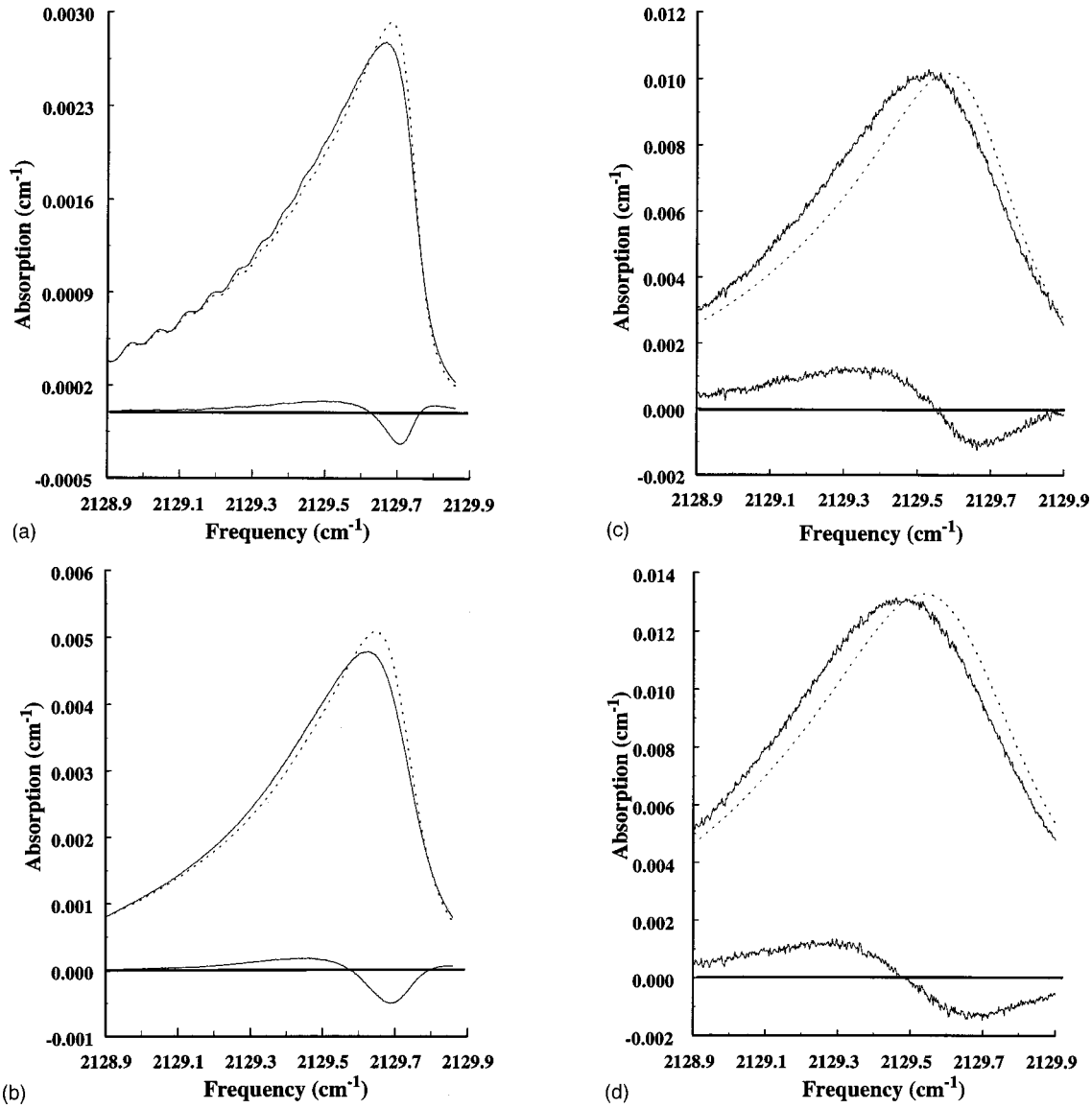

FIG. 9. A comparison of high pressure spectra (solid lines) of the 2130 cm^{-1} Q branch of CO_2 and spectra (dotted curves) predicted with no adjustable parameters from an EPG law that is fitted to low pressure difference frequency spectra. Also shown are the plots of the residuals. The spectra at (a) 1/2 atm and (b) 1 atm were recorded with the difference frequency spectrometer. The spectra at (c) 3 atm and (d) 5 atm were recorded with the FTIR spectrometer.

of the matrix equation for the band spectrum,[5,6] including in the calculated spectra the measured shifting of the Q branch and the simple overlap with neighboring P and R branch lines. Doppler broadening/Dicke narrowing and speed dependent broadening are safely ignored in the strong mixing limit. Note these are not fits to the high pressure spectra but are rather extrapolation of the low pressure spectra to pressures where strong mixing occurs at least among the low J lines, if not the entire Q branch. At this level of mixing our calculations are insensitive to the choice of the broadening coefficients, γ or $\overline{\gamma}$ that are used to determine the EPG parameters.

We see clearly, from the plot of the residuals in Fig. 9, that there is an asymmetric component which becomes increasingly larger with increasing pressure, although not linearly at the highest pressures. If mixing within the Q branch was all that mattered, then the asymmetry should decrease with increasing pressure. Another disturbing feature is the overall shift of the Q branch. The apparent shifting coefficient is negative, being about four times larger and of opposite sign to that measured at low pressures. If only the data above 3 atm were available, it would be tempting to shift the computed spectra to lower frequencies. While such a shift would reduce the overall size of the residual near the peak of the branch it would however produce a significant mismatch between the structure which is evident for the high J lines at 1 atm. It is this structure which fixes the two frequency scales.

We are therefore forced to conclude that the model is deficient in that it cannot predict the asymmetry of the band with increasing pressure and we must consider what physics is being ignored or poorly represented in the model. As suggested above, one immediate candidate is interbranch mixing which in this case is primarily between the Q and the P branch since the R branch is suppressed by Coriolis interactions.[30] If interbranch mixing is indeed the main

source of the mismatch between the observed and calculated spectra, then our sum rule results indicate that it may not be ignored even at low pressures. Interbranch mixing is an active area of research[31–33] and it remains to be seen if it is possible to incorporate this effect into the present model. These calculations are being pursued. We must emphasize that we have by no means proved that interbranch mixing is the main or sole source of the problem. Our calculations also ignore mixing within the *P* branch. It is clear from Fig. 1(b) that such mixing is strong above 3 atm since structure in this branch is beginning to disappear at such a pressure. No structure is observable in the *P* branch at 7 atm.

CONCLUSION

In summary we have measured, at pressures below 15 kPa, the line and branch strengths, and the broadening, mixing and band shifting coefficients for the *Q* branch of CO_2 situated at 2130 cm^{-1}. The data have been analyzed using two different line shape models, V_{wm}, a speed independent Voigt that included weak line mixing and HC_v, a speed dependent hard collision model that also included line mixing. It has been found that the HC_v model best represents our data. Where appropriate, we have compared our results with experimental values available in the literature. Measurements made at pressures above 15 kPa, and up to 2000 kPa (20 atm) strongly indicate that interbranch mixing with the *P* branch may not be ignored. At low pressures ($P<15$ kPa) it will affect the line asymmetry and cause the weak mixing sum rule to be violated.

ACKNOWLEDGMENTS

This work was supported by funding from the Natural Sciences and Engineering Research Council of Canada, COMDEV, Bomem Inc., Atmospheric Environment Service, University of Toronto Research Fund and the Canadian Space Agency. Our gratitude also goes to Cyril Hnatovsky for his help with the design of the 4 m cell and to J. P. Bouanich, C. Boulet, and J. M. Hartmann for numerous fruitful discussions.

[1] C. D. Rogers, Rev. Geophys. Space Phys. **14**, 609 (1976).
[2] R. Berman, P. M. Sinclair, A. D. May, and J. R. Drummond, J. Mol. Spectrosc. **197**, 283 (1999).
[3] L. S. Rothman *et al.*, J. Quant. Spectrosc. Radiat. Transf. **48**, 469 (1992).
[4] M. Baranger, Phys. Rev. **111**, 494 (1958); **111**, 481 (1958); **112**, 855 (1958).
[5] A. Levi, N. Lancome, and C. Chackerian, Jr., *Collisional Line Mixing*, edited by K. N. Rao and A. Weber (Academic, New York, 1992), p. 261.
[6] A. D. May, Phys. Rev. A **59**, 3495 (1999).
[7] E. W. Smith, J. Chem. Phys. **74**, 6658 (1981).
[8] L. L. Strow and B. M. Gentry, J. Chem. Phys. **84**, 1149 (1986).
[9] D. Edwards and L. L. Strow, J. Geophys. Res. D **96**, 20859 (1991).
[10] P. W. Rosenkranz, IEEE Trans. Antennas Propag. **AP-23**, 498 (1975).
[11] B. M. Gentry and L. L. Strow, J. Chem. Phys. **86**, 5722 (1987).
[12] A. Henry, D. Hurtmans, M. Margotin-Maclou, and A. Valentin, J. Quant. Spectrosc. Radiat. Transf. **56**, 647 (1996).
[13] R. Berman, P. Duggan, P. M. Sinclair, A. D. May, and J. R. Drummond, J. Mol. Spectrosc. **182**, 350 (1997).
[14] A. Predoi-Cross, Caiyan Luo, P. M. Sinclair, J. R. Drummond, and A. D. May, J. Mol. Spectrosc. **198**, 291 (1999).
[15] P. Duggan, P. M. Sinclair, M. P. Le Flohic, J. W. Forsman, R. Berman, A. D. May, and J. R. Drummond, Phys. Rev. A **48**, 2077 (1993).
[16] R. Berman, Ph.D. thesis, Dept. of Physics, University of Toronto, 1998.
[17] S. Green, J. Chem. Phys. **90**, 3603 (1989).
[18] S. G. Rautian and I. I. Solbelman, Sov. Phys. J. **9**, 701 (1967).
[19] T. Marrero and E. A. Mason, J. Phys. Chem. Ref. Data **1**, 3 (1972).
[20] B. Lavorel *et al.*, J. Chem. Phys. **93**, 2185 (1990).
[21] R. Berman, P. M. Sinclair, A. D. May, and J. R. Drummond, J. Mol. Spectrosc. **198**, 278 (1999).
[22] L. S. Rothman *et al.*, J. Quant. Spectrosc. Radiat. Transf. **60**, 665 (1998).
[23] C. P. Rinsland, D. C. Benner, and V. Malathy Devi, Appl. Opt. **25**, 1204 (1986).
[24] L. S. Rothman *et al.*, Appl. Opt. **22**, 2247 (1983).
[25] V. Dana *et al.*, J. Quant. Spectrosc. Radiat. Transf. **52**, 333 (1994).
[26] J. W. C. Johns, J. Mol. Spectrosc. **125**, 442 (1987).
[27] L. L. Strow, D. C. Tobin, and S. E. Hannon, J. Quant. Spectrosc. Radiat. Transf. **52**, 281 (1994).
[28] L. L. Strow and D. Reuter, Appl. Opt. **27**, 872 (1988).
[29] Equation (2) of R. Rodriques and J-M. Hartmann [J. Quant. Spectrosc. Radiat. Transf. **57**, 63 (1997)] emphasizes that the usual form of the sum rule ignores certain frequency factors. Such factors should be included in the analysis of the spectra and in testing the sum rule. We have ignored them here.
[30] G. Herzberg, *Infrared and Raman Spectra of Polyatomic Molecules* (Van Nostrand Reinhold Company, New York, 1945).
[31] M. V. Tonkov, N. N. Filippov, Yu. M. Timofeyev, and A. V. Polyakov, J. Quant. Spectrosc. Radiat. Transf. **56**, 783 (1996).
[32] L. Ozanne *et al.*, J. Quant. Spectrosc. Radiat. Transf. **58**, 261 (1997).
[33] J-M. Hartmann, R. Rodrigues, Nguyen-Van-Thanh, C. Broddbeck, and C. Boulet, J. Chem. Phys. **110**, 7733 (1999).